Available online at www.sciencedirect.com

SCIENCE DIRECT®

International Journal of Heat and Fluid Flow 26 (2005) 801–809

International Journal of HEAT AND FLUID FLOW

www.elsevier.com/locate/ijhff

# Flow boiling heat transfer of carbon dioxide in horizontal mini tubes

Rin Yun [a], Yongchan Kim [a,*], Min Soo Kim [b]

[a] Department of Mechanical Engineering, Korea University, Anam-dong, Sungbuk-ku, Seoul 136-701, Republic of Korea
[b] Department of Mechanical and Aerospace Engineering, Seoul National University, Seoul 151-744, Republic of Korea

Received 1 July 2004; received in revised form 12 January 2005; accepted 19 January 2005
Available online 25 March 2005

**Abstract**

Flow boiling heat transfer coefficients of carbon dioxide ($CO_2$) in mini tubes with inner diameters of 2.0 and 0.98 mm are measured and analyzed as a function of operating parameters. The heat transfer coefficients are measured at high mass fluxes from 500 to 3570 kg/m$^2$ s, heat fluxes from 7 to 48 kW/m$^2$, and saturation temperatures of 0, 5 and 10 °C. The measured heat transfer coefficients before dryout are in the range of 10 000–20 000 W/m$^2$ K. The heat transfer coefficients before critical vapor quality are strongly affected by heat flux at all mass flux conditions. However, the effects of mass flux on heat transfer coefficients before critical vapor quality are only significant when the superficial liquid Weber number is less than 100. The heat transfer characteristics after critical vapor quality are explained by partially dried liquid film and rate of liquid droplets in the vapor core. Based on the database obtained from this study and the literature, a boiling heat transfer correlation before critical vapor quality is developed.


*Keywords:* Boiling heat transfer; Carbon dioxide ($CO_2$); Mini tubes; Correlation

## 1. Introduction

Carbon dioxide ($CO_2$) has been reintroduced as a potential working fluid of automobile air-conditioners, water heater heat pumps, and residential air conditioners due to increasing environmental concerns. Improving efficiency of a transcritical $CO_2$ cycle for these systems to an equivalent level of a conventional HCFC or CFC system is a primary concern of current research. In order to enhance the performance of a heat exchanger, the $CO_2$ system uses a microchannel heat exchanger or a compact heat exchanger made up with mini tubes due to its higher volumetric heat capacity and lower pressure drop. In addition, the development of a compact and efficient heat exchanger using conventional refrigerants has received significant interest due to its wide applications to the chemical processing and cooling of electronic equipment. Therefore, the understanding of two-phase heat transfer characteristics of $CO_2$ in mini tubes is very essential to develop a compact heat exchanger appropriate for the transcritical cycle.

The boiling heat transfer coefficients of water and conventional refrigerants in small tubes and channels have been investigated by many researchers. Lazarek and Black (1982), Bao et al. (2000), Yu et al. (2002), and Wambsganss et al. (1991) reported that the heat transfer coefficients were fully controlled by heat flux due to retarded suppression of nucleate boiling at a high Boiling number and the large slug flow regime in a small channel. Qu and Mudawar (2003), Sumith et al. (2003), and Yan and Lin (1998) emphasized the dominant role of mass flux in the boiling heat transfer. Kew and Cornwell (1997) showed that intermittent dryout occurred under a wider range of operating conditions than expected, and the heat transfer mechanism became much more complex with a decrease of tube diameter.

* Corresponding author. Tel.: +82 2 3290 3366; fax: +82 2 921 5439.
*E-mail address:* yongckim@korea.ac.kr (Y. Kim).

0142-727X/$ - see front matter © 2005 Elsevier Inc. All rights reserved.
doi:10.1016/j.ijheatfluidflow.2005.01.004

**Nomenclature**

| | |
|---|---|
| $Bo$ | Boiling number |
| $D$, $d_h$ | inner tube diameter, hydraulic (m) |
| $G$ | mass flux (kg/m$^2$ s) |
| $h$ | two-phase heat transfer coefficient (W/m$^2$ K) |
| $i$ | enthalpy (kJ/kg), number index |
| $j$ | superficial velocity (m/s) |
| $k$ | thermal conductivity (W/m K) |
| $M$ | molecular mass (kg/mol) |
| $n$ | number of data |
| $Pr$ | Prandtl number |
| $p_r$ | reduced pressure |
| $R_p$ | surface roughness parameter (μm) |
| $q$ | heat flux |
| $S$ | standard deviation |
| $T_e$ | evaporating temperature (°C, K) |
| $U$ | uncertainty |
| $u$ | velocity (m/s) |
| $We$ | Weber number |
| $x$ | vapor quality |

*Greeks*

| | |
|---|---|
| $\rho$ | density (kg/m$^3$) |
| $\Delta\rho$ | density difference between phases (kg/m$^3$) |
| $\mu$ | dynamic viscosity (Ns/m$^2$) |
| $\delta$ | liquid film thickness (m) |
| $\sigma$ | surface tension (N/m) |

*Subscripts*

| | |
|---|---|
| cr | critical |
| e | equilibrium |
| f, l | liquid phase |
| o | reference |
| p | preheater |
| r | refrigerant |
| s | superficial |
| t | test section |
| v | vapor |
| w | wall |

Several researchers have also performed on the boiling heat transfer characteristics of $CO_2$ in mini tubes or channels of which hydraulic diameters were approximately 1.0 mm. Pettersen (2004) investigated flow vaporization of $CO_2$ in a microchannel tube. He showed that critical vapor quality decreased and a steeper degradation of the heat transfer coefficient occurred at high mass fluxes and high saturation temperatures. Hihara and Tanaka (2002) measured boiling heat transfer coefficients and pressure drops of $CO_2$ in a smooth round tube having an inner diameter of 1.0 mm. Critical vapor quality, causing a rapid drop of heat transfer coefficient, was significantly affected by mass flux. Neksa and Pettersen (2001) measured boiling heat transfer coefficient and pressure drop in microchannels and then calculated critical vapor quality using the Ahmad method (Ahmad, 1973). Zhao et al. (2001) compared test data of $CO_2$ in microchannels with the Liu and Winterton correlation that was developed for a conventional sized tube. They suggested that the Liu and Winterton correlation has to be revised by considering a confinement factor.

Generally, nucleate boiling plays a dominant role in two-phase flow heat transfer in mini tubes. However, the effects of major operating parameters such as heat flux and mass flux on the boiling heat transfer of $CO_2$ in mini tubes have not been sufficiently explained in the previous studies. The objectives of this study are to investigate boiling heat transfer characteristics of $CO_2$ in mini tubes and to develop a heat transfer correlation for pre-critical vapor quality based on a wide range of experimental database. The heat transfer coefficients of $CO_2$ in mini tubes are measured and then analyzed as a function of heat flux, mass flux, and vapor quality. The effects of mass flux are also theoretically studied by using flow patterns developed in mini channels. Based on the database obtained from this study and the literature, the boiling heat transfer correlation before critical vapor quality is developed.

## 2. Experimental setup and test conditions

As shown in Fig. 1, the experimental setup used in this study consists of a magnetic gear pump, a mass flow meter, a preheater, a test section, and a plate heat exchanger. The gear pump circulates $CO_2$ and the preheater controls inlet vapor quality of the test section. Two-phase $CO_2$ at the exit of the test section is completely condensed and subcooled by using the plate heat exchanger operated with a chiller. Using a control tank that is kept inside of a constant temperature bath regulates charge amount of $CO_2$ in the test setup.

The test tubes used in this study are smooth tubes with inner diameters (ID) of 2.0 mm and 0.98 mm, which are made of stainless steel. The outside diameters are 3.2 mm and 1.6 mm, and the heated lengths are 1200 mm and 400 mm for the 2.0 mm and 0.98 mm ID tube, respectively. Applying a direct heating method provides heat flux to the test section. A high-current transformer with a maximum current and voltage of 120 A and 20 V is used to supply heat flux. Thermocouples are placed on the top and the bottom of each measuring point, which is equally located along the test

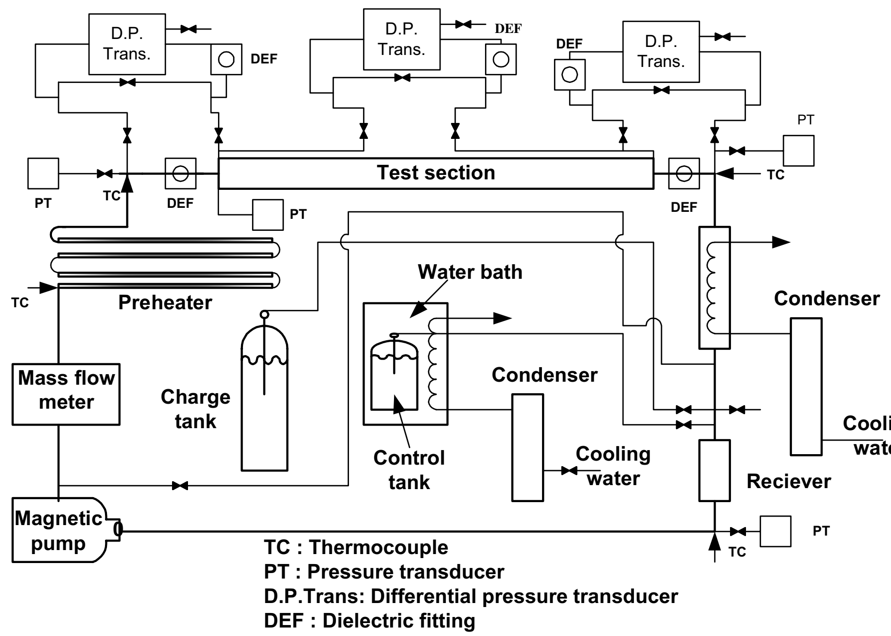


Fig. 1. Schematic of the experimental setup.

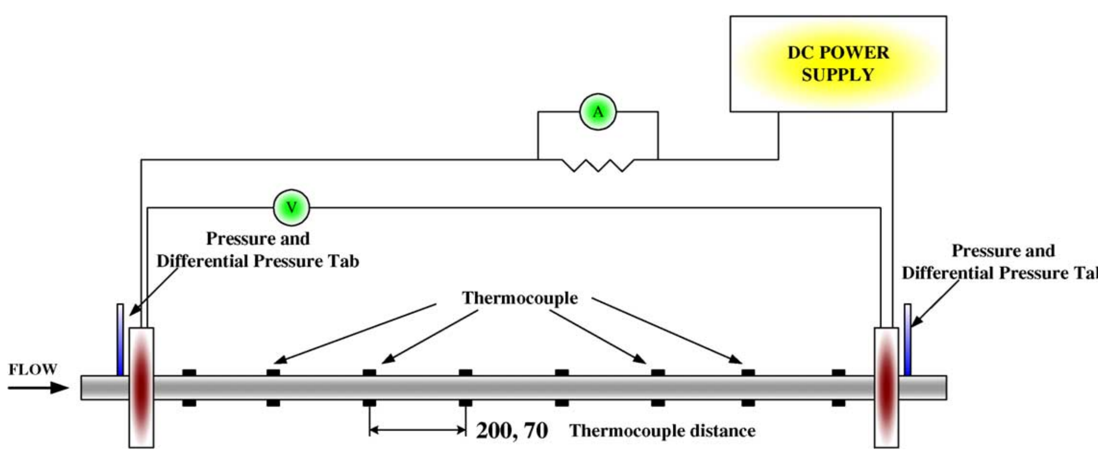


Fig. 2. Details of the test section.

section with an interval of 200 mm for the 2.0 mm ID tube, and 70 mm for the 0.98 mm ID tube as shown in Fig. 2. The thermocouple junctions are electrically insulated from the tube using a very thin Teflon tape. The test section is insulated using a rubber with a thermal conductivity of 0.04 W/m K to minimize heat exchange to ambient. The heat loss is estimated by comparing electric heat input with actual heat transfer rate to the working fluid, which is calculated in terms of the enthalpy difference across the test section in subcooled state. The heat loss in the preheater and the test section is taken into account in the calculations of vapor quality and heat transfer coefficient.

The refrigerant flow rate is measured using a Coriolis effect flow meter with an uncertainty of a ±0.2% reading. All temperatures are measured using T-type thermocouples with a calibrated accuracy of ±0.1 °C. The temperature differences among the thermocouples during single-phase runs are less than ±0.2 °C. The pressure of the refrigerant entering the test section is monitored with a pressure transducer with an uncertainty of ±2.1 kPa, while the pressure drop across the test section is measured with a strain-gage-type differential pressure transducer. The power inputs to the preheater and the test section are monitored using a watt transducer with an uncertainty of ±0.2% on full scale.

The test conditions for each tube are shown in Table 1. For the 0.98 mm ID tube, the tests are conducted at mass fluxes from 1000 kg/m$^2$ s to 2000 kg/m$^2$ s, heat fluxes from 20 kW/m$^2$ to 40 kW/m$^2$, and saturation temperatures from 0 °C to 10 °C. For the

Table 1
Test conditions

| Tube diameter (mm) | Saturation temperature (°C) | Heat flux ($kW/m^2$) | Mass flux ($kg/m^2$ s) |
|---|---|---|---|
| 0.98 | 0 | 20, 30 | 1500.0 |
| | 5 | 20, 30, 40 | 1000.0 |
| | | 20, 30, 40 | 1500.0 |
| | | 20, 30, 40 | 2000.0 |
| | 10 | 20, 30 | 1500.0 |
| 2.0 | 5 | 7.9, 26 | 500 |
| | | 7.2, 15.9, 26.5, 36.0, 46.0 | 1000 |
| | 5 | 7.3, 16.2, 20.0, 26.0, 30.0, 36.0 | 1786.0 |
| | | 17.3, 24.5, 31.7, 37.1 | 2381.0 |
| | | 15.9, 24.5, 37.5, 48.1 | 2976.0 |
| | | 17.5, 26.7, 37.7, 47.4 | 3571.0 |
| | 10 | 18.4 | 595.3 |

2.0 mm ID tube, mass flux is varied from 500 $kg/m^2$ s to 3570 $kg/m^2$ s, while heat flux is altered from 7 $kW/m^2$ to 48 $kW/m^2$ at saturation temperatures of 5 °C and 10 °C.

The heat transfer coefficient, $h$, of $CO_2$ inside a smooth tube is determined from the measured heat flux, $q$, the refrigerant temperature, $T_r$, and the calculated inside wall temperature, $T_w$. The $T_w$ is calculated from the measured outside wall temperatures using the equation of steady-state radial heat conduction through the tube.

$$h = \frac{q}{(T_w - T_r)} \tag{1}$$

The refrigerant temperatures of $T_r$ at each axial position are determined by using an interpolation method with an assumption of a linear temperature gradient in the bulk fluid over the heated length.

Uncertainties of the present experiments are analyzed with RRS method suggested by Moffat (1985). The final uncertainties are estimated by averaging the uncertainties calculated at all test conditions. During the averaging process, the uncertainties located upper 2.5% and lower 2.5% are discarded with the assumption of normal distribution of uncertainties. Therefore, the final uncertainties are located within 95% of reliability. The calculation procedures for the uncertainties are provided in Appendix A. The results from the present uncertainty analysis for the experiments are summarized in Table 2.

Table 2
Parameters and estimated uncertainties

| Parameters | Uncertainty |
|---|---|
| Temperature | ±0.1 °C |
| Pressure | ±2.1 kPa |
| Measured pressure drop | ±52 Pa |
| Mass flow of refrigerant | ±0.2% |
| Heat transfer rate of test section | ±5% |
| Vapor quality at the inlet of test section | ±0.04 |
| Evaporation heat transfer coefficient | ±9.5% |

## 3. Results and discussion

### 3.1. Boiling heat transfer coefficients with vapor quality

Fig. 3 shows the heat transfer coefficients of $CO_2$ with respect to vapor quality in the 2.0 mm ID tube at a mass flux of 1000 $kg/m^2$ s and a saturation temperature of 5 °C. For a lower heat flux (7.2 $kW/m^2$), the heat transfer coefficient gradually increases with a rise of vapor quality. When the heat flux increases beyond 15.9 $kW/m^2$, a rapid reduction of the heat transfer coefficient is observed at a critical vapor quality. This trend would be due to the formation of dryout patches near the tube wall at a critical heat flux (CHF). Generally, before the critical vapor quality, the heat transfer coefficients significantly increase with a rise of heat flux due to an enhancement of nucleate boiling. However, after the critical vapor quality, the heat transfer coefficients are merged together regardless of heat flux, and the effects of heat flux become negligible. As shown in Fig. 3, the critical vapor quality decreases with a rise of heat flux, but it remains nearly constant when the heat flux becomes larger.

Fig. 4 shows the heat transfer coefficients for $CO_2$ in the 2.0 mm ID tube at a mass flux of 1500 $kg/m^2$ s and a saturation temperature of 5 °C. The dryout phenomenon exists when the heat flux is greater than 26 $kW/m^2$, which is higher than the critical heat flux (15.9 $kW/m^2$) at a mass flux of 1000 $kg/m^2$ s. Generally, critical vapor quality and CHF become larger when mass flux increases beyond a specific limit of transition mass flux. This transition mass flux was also found in steam–water CHF table, but it was larger than that of the present data. This difference in the transition mass flux between them may be due to the better wettability of $CO_2$ than that of steam–water (Yun and Kim, 2003). In this study, the CHF is determined when the wall temperature sharply increases and the heat transfer coefficient drops significantly. After the critical vapor quality at a lower mass flux (Fig. 3), the heat transfer

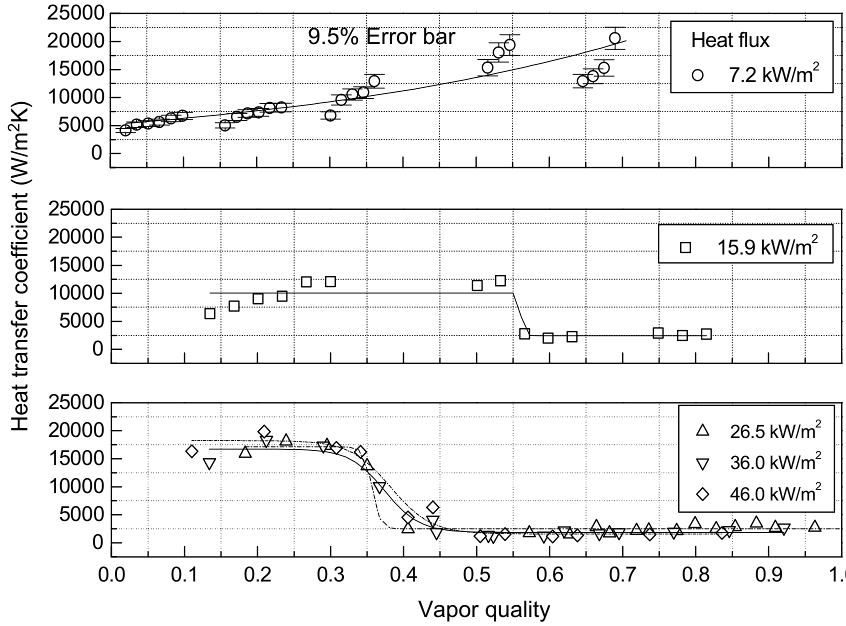


Fig. 3. Heat transfer coefficients for the 2.0 mm ID tube at a mass flux of 1000 kg/m$^2$ s and saturation temperature of 5 °C.

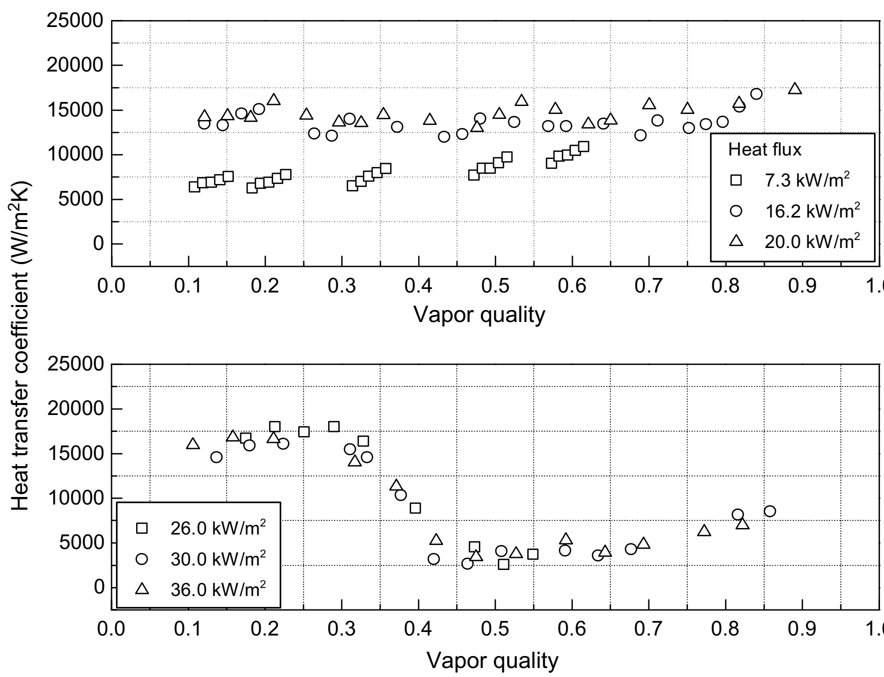


Fig. 4. Heat transfer coefficients for the 2.0 mm ID tube at a mass flux of 1500 kg/m$^2$ s and saturation temperature of 5 °C.

coefficient sharply drops and then remains nearly constant. However, for a mass flux of 1500 kg/m$^2$ s (Fig. 4), the heat transfer coefficient rapidly decreases at critical vapor quality, and then gradually increases with a rise of vapor quality. These trends were also observed in the experiments with steam–water mixture (Groeneveld and Delorme, 1976). It should be noted that this tendency become more significant when the tube diameter is small, mass flux is very high, and the surface tension of fluid is very small. Generally, the collision of liquid droplets in the vapor core to the wall becomes easier with a rise of mass flux, a reduction of surface tension, and a decrease of tube diameter due to an increase of liquid droplet concentration in the vapor core and a limited space of liquid droplet movement. Therefore, due to a higher collision rate of liquid droplets to the wall with deficient of liquid film (Hewitt, 1982) the heat transfer coefficient gradually increases after the dryout. However, the film distortion and liquid film dryout are significantly affected by heat flux.

Fig. 5 shows the comparison of the present data with Hihara and Tanaka (2002) data for the 0.98 mm ID tube. The saturation temperatures of Hihara and Tanaka (2002) and the present study are 15 °C and 10 °C, respectively. As observed in the 2.0 mm ID tube, the critical vapor quality for the 0.98 mm ID tube decreases with an increase of heat flux. The present and reference data show similar heat transfer coefficients before and after critical vapor quality. As the saturation temperature increases from 10 °C to 15 °C, the reduction of the heat transfer coefficient near critical vapor quality becomes significant. The bubble formation in the liquid sub-layer may increase with a rise of saturation temperature, which will cause more dry patches on the tube wall.

### 3.2. Boiling heat transfer characteristics before critical vapor quality

Because the boiling heat transfer coefficients of $CO_2$ in mini tubes are dramatically varied before and after critical vapor quality, it is necessary to develop two different heat transfer correlations for pre and post-critical vapor quality. However, this study focuses on the development of a heat transfer correlation before critical vapor quality due to limited results of heat transfer coefficients for post-critical vapor quality. The critical vapor qualities are predicted by using the theoretical annular flow model for $CO_2$ in mini tubes (Yun and Kim, 2003). A database for the present heat transfer correlation before critical vapor quality is obtained from this study, Hihara and Tanaka (2002), and Neksa and Pettersen (2001). Table 3 shows the detailed information on the present database including data range and number of data points. It should be noted that Tran et al.'s data (Tran et al., 1995) were only used in the data comparison. The database covers tube diameters from 0.79 to 2.0 mm, heat fluxes from 5 to 48.1 kW/m$^2$, and mass fluxes from 190 to 3571 kg/m$^2$ s.

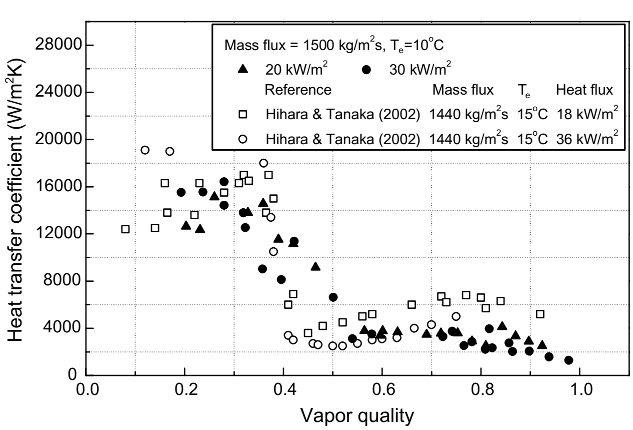


Fig. 5. Heat transfer coefficients for the 0.98 mm ID tube.

When mass flux is less than 500 kg/m$^2$ s, the heat transfer coefficients are positively proportional to mass flux by the Pearson's correlation coefficient of 0.62. The Pearson's correlation coefficient is defined as Eq. (2). The value of 0.62 indicates that $h$ and $G$ have close positive relationship.

$$r = \frac{\sum_{i=1}^{n}(h_i - \bar{h})(G_i - \bar{G})}{(n-1)S_h S_G} \tag{2}$$

However, when mass flux is greater than 500 kg/m$^2$ s, there is no distinct relationship between heat transfer coefficients and mass flux.

Fig. 6 shows that the heat transfer coefficients are strongly dependent on heat flux at all mass flux conditions. Besides, the effects of heat flux are significantly varied according to working fluids. It should be noted that 10% of the data for $CO_2$, which had large data scattering occurred by some errors in the evaluation of critical vapor quality, were selectively discarded. The heat transfer coefficients of $CO_2$ are proportional to $q^{0.72}$, while those of R113, R12 and R134a are proportional to $q^{0.62}$ (Tran et al., 1995). Therefore, when mass flux is lower than a certain limit, it is required to simultaneously apply the terms of mass flux and heat flux in the heat transfer correlation. However, when mass flux is greater than the limit, it may be sufficient to apply only heat flux in the heat transfer correlation. In this study, the mass flux limit in the application of the correlation is determined by using a superficial liquid Weber number, $We_{ls}$.

$$We_{ls} = \rho j_l^2 d_h / \sigma \tag{3}$$

When $We_{ls}$ is less than 100, flow experiences three different flow regimes: bubbly, slug, and annular (Yun and Kim, 2004). Slugs or confined bubbles occupy large portion of a mini tube at low mass flux conditions. The packed bubbles in a mini tube cause flow instability and flow fluctuation, which can increase heat transfer coefficient in this unstable region with an increase of flow rate (Brutin and Tadrist, 2004). Therefore, both mass flux and heat flux are dominant parameters in the determination of the heat transfer coefficients when $We_{ls} < 100$.

When $We_{ls}$ is greater than 100, the flow regime transits directly from bubbly to annular flow without having slug flow (Yun and Kim, 2004). Liquid droplets in the vapor core and the deposition of the liquid droplets into the liquid film in a limited space increase simultaneously with a rise of mass flux, which may cause a degradation of effective film evaporation in a mini tube. In addition, the liquid film thickness can be maintained at enough level for nucleate boiling by active deposition of liquid droplets at high mass fluxes. Therefore, the effects of

Table 3
Data sources used in this study

| Reference | Working fluid | $q$ (kW/m$^2$) | $G$ (kg/(m$^2$ s)) | $p_r$ | Tube geometry (ID(mm)) | Number of exp. data |
|---|---|---|---|---|---|---|
| | | | | | | Before $x_{cr}$ |
| Present study | $CO_2$ | 7.2–48.1 | 500–3571.0 | 0.47–0.61 | Circular (2.0, 0.98) | 498 |
| Hihara and Tanaka (2002) | $CO_2$ | 9–36 | 360–1440 | 0.69 | Circular (1.0) | 155 |
| Neksa and Pettersen (2001) | $CO_2$ | 5–20 | 190–570 | 0.47–0.87 | Circular channel (0.79) | 88 |
| Tran et al. (1995)[a] | R-12 | 2.22–128.6 | 44–832 | 0.12, 0.20 | Circular (2.92, 2.46) | 363 |
| | R-113 | | | 0.045 | Rectangular (4.06 × 1.70) | |
| | R-134a | | | 0.10, 0.20 | | |

[a] The data are used only for the comparison, not for the database of the present correlation.

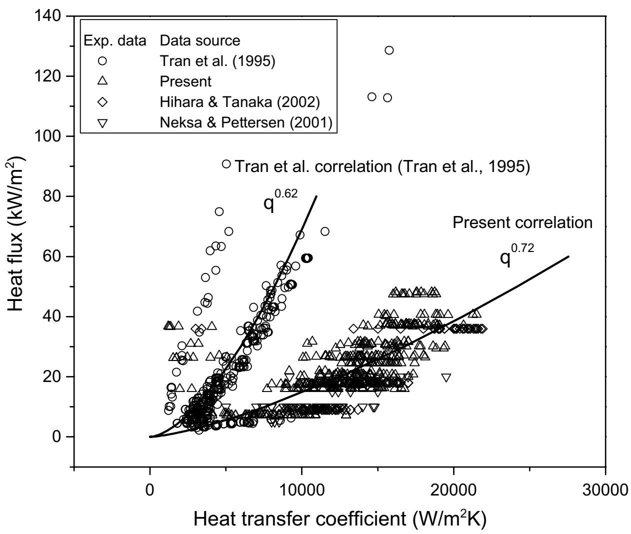


Fig. 6. Effects of heat flux on heat transfer coefficients before critical vapor quality.

mass flux become insignificant as compared to those of heat flux when $We_{ls}$ increases beyond 100 in mini tubes. The heat flux strongly affects the heat transfer coefficients in mini tubes regardless of $We_{ls}$.

Based on the data analysis for the database as shown in Table 3, it was observed that approximately 85% of the superficial liquid Weber numbers for $CO_2$ in mini tubes was greater than 100. Therefore, a correlation before critical vapor quality is generated from a power law form of heat flux and reduced pressure. The basic form of the correlation is similar to the Borishanski correlation (Borishanski, 1969) that was developed for nucleate boiling with steam/water and air/water mixtures. After determining the coefficient and exponents of the correlation using a non-linear regression analysis based on the database, the final correlation before critical vapor quality in mini tubes using $CO_2$ is given as

$$h = 16.26 q^{0.72} p_r^{0.88} \tag{4}$$

Table 4 compares the predicted results of the present correlation, the Cooper correlation (Cooper, 1984), the Gorenflo correlation (Gorenflo, 1993), the Liu and Winterton correlation (Liu and Winterton, 1991) with the present database for $CO_2$. The Cooper and the Gorenflo correlation considers heat flux, reduced pressure, and surface roughness as dominant variables, which are very similar to those of the present correlation. The Liu and Winterton correlation shows a mean deviation of 42% with the measured data. The present correlation shows better predictions than other existing correlations. The present correlation yields a mean deviation of 38% and average deviation of 10% based on the present database. Some of large deviations are due to uncertainties in the prediction of critical vapor quality. It should be noted that the Cooper and the Gorenflo correlations were developed for nucleate pool boiling and the Liu and Winterton correlation included the Cooper correlation in the calculation of the nucleate boiling term.

### 3.3. Boiling heat transfer characteristics after critical vapor quality

The interfacial evaporation of liquid film and liquid droplets in the vapor core, and superheating of vapor

Table 4
Comparison of the present correlation with the existing correlations before critical vapor quality

| Reference | Correlation | Mean dev.[a] | Ave dev.[b] |
|---|---|---|---|
| Present study | $h = 16.26q^{0.72}p_r^{0.88}$, $q$ (W/m$^2$) | 38% | −10% |
| Cooper (1984) | $h = 55p_r^{0.12}(-\log_{10}p_r)^{-0.55}M^{-0.5}q^{0.67}$ | 38% | −18% |
| Gorenflo (1993) | $h = h_o F_{PF}(q/q_o)^{nf}(R_p/R_{po})^{0.133}$, $h_o = 4170$ ($CO_2$) | 48% | −40% |
| | $F_{PF} = (1.2p_r^{0.27} + (2.5 + 1/(1-p_r))p_r)$, $q_o = 20$ kW/m$^2$, $R_{po} = 0.4$ μm | | |
| Liu and Winterton (1991) | $h = ((Eh_{\text{Dittus-Boelter}})^2 + (Sh_{\text{Cooper}})^2)^{1/2}$ | 42% | −28% |

[a] Mean dev. $= \frac{1}{n}\sum_1^n \text{ABS}[((h_{exp} - h_{pred}) \times 100)/h_{exp}]$.
[b] Ave dev. $= \frac{1}{n}\sum_1^n [((h_{exp} - h_{pred}) \times 100)/h_{exp}]$.

core can determine the heat transfer characteristics after critical vapor quality. Partially dried liquid film plays an important role in the post dryout heat transfer, and partially torn liquid film continually interacts with the deposited liquid droplets. The effects of liquid droplets on the heat transfer coefficients in a mini tube are much more significant than those in a large diameter tube due to the restriction of the movement of liquid droplets in the confined space of a mini tube.

In this study, the heat transfer correlation after critical vapor quality is not developed due to a limited data range for post-critical vapor quality. Further study is required to obtain more extensive heat transfer data enough to develop a generalized heat transfer correlation after critical vapor quality.

## 4. Conclusions

In this study, the boiling heat transfer characteristics of $CO_2$ in the mini tubes are experimentally investigated. The heat transfer coefficients of $CO_2$ are varied with heat flux and mass flux conditions and significantly reduced at critical vapor quality. The effects of heat flux on the heat transfer coefficient before critical vapor quality are very strong at all mass fluxes. However, the effects of mass flux on the heat transfer coefficient before critical quality are only significant when the mass flux is less than 500 kg/m$^2$ s, which value is generalized by a superficial liquid Weber number of 100. Based on the database for $CO_2$ obtained from this study and the literature, the heat transfer correlation before critical vapor quality in mini tubes is generated from a power law form of heat flux and reduced pressure. The heat transfer characteristics after critical vapor quality in mini tubes are explained by interactions between liquid droplets and the tube wall, which play an important role in the determination of dryout phenomena.

## Acknowledgments

This work was jointly supported by the Korea Science and Engineering Foundation (Grant No. R01-2002-000-00481-0), and the Carbon Dioxide Reduction and Sequestration Center, one of the 21st Century Frontier R&D Programs in the Ministry of Science and Technology of Korea.

## Appendix A. Uncertainty analysis

### A.1. Principles of uncertainty analysis

When $R$ is the function of independent variables, $x_1$, $x_2,\ldots,x_n$ and $U_1$, $U_2,\ldots,U_n$ are defined as the uncertainty of each independent variable. The uncertainty of $R$ can be calculated with Eq. (A.1.1) at each test conditions. The uncertainty is estimated by averaging the uncertainties calculated at each test conditions, which are located within 95% of reliability

$$U_R = \left[\left(\frac{\partial R}{\partial x_1}U_1\right)^2 + \left(\frac{\partial R}{\partial x_2}U_2\right)^2 + \cdots + \left(\frac{\partial R}{\partial x_n}U_n\right)^2\right]^{\frac{1}{2}} \tag{A.1.1}$$

### A.2. Uncertainty of the heat transfer coefficient

The uncertainties of the heat transfer coefficients are defined as Eq. (A.2.1). The uncertainties of $U_q$, $U_{T_r}$, and $U_{T_w}$ are shown in Table 2

$$\frac{U_h}{h} = \left[\left(\frac{1}{q}U_q\right)^2 + \left(-\frac{U_{T_r}}{(T_w - T_r)}\right)^2 + \left(\frac{U_{T_w}}{(T_w - T_r)}\right)^2\right]^{\frac{1}{2}} \tag{A.2.1}$$

### A.3. Uncertainty of vapor quality at the inlet of the test section

As shown in Eq. (A.3.1), the vapor qualities at the inlet of the test section are calculated based on enthalpy and fluid temperatures at the inlet of the test section. The uncertainty of vapor quality is defined as Eq. (A.3.2). Eqs. (A.3.3 and A.3.4) show the uncertainties of $U_{i_{t,i}}$, $U_{i_f}$, and $U_{i_{fg}}$.

$$x = x(i_{t,i}, T_r) = (i_{t,i} - i_f)/i_{fg} \tag{A.3.1}$$

$$\frac{U_x}{x} = \sqrt{\left(\frac{\frac{1}{i_{fg}}U_{i_{t,i}}}{\frac{i_{t,i}-i_f}{i_{fg}}}\right)^2 + \left(\frac{-\frac{1}{i_{fg}}U_{i_f}}{\frac{i_{t,i}-i_f}{i_{fg}}}\right)^2 + \left(-\frac{1}{i_{fg}}U_{i_{fg}}\right)^2} \tag{A.3.2}$$

$$U_{i_{t,i}} = i_{t,i}\sqrt{\left(\frac{1}{i_p + \frac{q}{G}}\right)^2\left(\frac{\partial i_p}{\partial T_f}U_{T_f}\right)^2 + \left(\frac{\frac{1}{G}}{i_p + \frac{q}{G}}\right)^2 U_q^2 + \left(\frac{-\frac{q}{G^2}}{i_p + \frac{q}{G}}\right)^2 U_G^2}$$

$$i_{t,i} = i_p + q/G, \qquad i_p, i_f, i_{fg} = i(T_r) \tag{A.3.3}$$

$$U_{i_f} = \frac{\partial i_f}{\partial T_f} U_{T_f}$$

$$U_{i_{fg}} = \frac{\partial i_{fg}}{\partial T_r} U_{T_r} \tag{A.3.4}$$

## References


Ahmad, S.Y., 1973. Fluid to fluid modeling of critical heat flux: A compensated distortion model. Int. J. Heat Mass Transfer 16, 641–662.

Bao, Z.Y., Fletcher, D.F., Haynes, B.S., 2000. Flow boiling heat transfer of in narrow passages Freon R11 and HCFC123. Int. J. Heat Mass Transfer 43, 3347–3358.

Borishanski, V.M., 1969. Correlation of the effect of pressure on the critical heat flux and heat transfer rates using the theory of thermodynamics similarity. In: Problems of Heat Transfer and Hydraulics of Two-phase Media. Pergamon Press, pp. 16–37.

Brutin, D., Tadrist, L., 2004. Pressure drop and heat transfer analysis of flow boiling in a minichannel: Influence of the inlet condition on two-phase flow stability. Int. J. Heat Mass Transfer 47, 2365–2377.

Cooper, M.C., 1984. Heat flow rates in saturated nucleate pool boiling—a wide ranging examination using reduced properties. In: Irvine, F., Thomas (Eds.), Advances in Heat Transfer. Academic Press, Orlando, pp. 157–239.

Gorenflo, D., 1993. Pool boiling. In: VDI Gesellschaft Verfahrenstechnic und Chemieingenieurwesen (Ed.). English translation of VDI, Düsseldorf, Ha 4–Ha 18.

Groeneveld, D.C., Delorme, G.G.J., 1976. Prediction of thermal non-equilibrium in the post-dryout regime. Nucl. Eng. Design 36, 17–26.

Hewitt, G.F., 1982. Pressure drop. In: Hetsroni G. (Ed.), Handbook of Multiphase System. Hemisphere Publishing Corporation, Washington DC, 2-44–2-75.

Hihara, E., Tanaka, S., 2002. Boiling heat transfer of carbon dioxide in horizontal tubes. In: Proc. 4th IIR-Gustav Lorentzen Conf. Natural Working Fluids, Purdue, 279–284.

Kew, P.A., Cornwell, K., 1997. Correlations for the prediction of boiling heat transfer in small-diameter channels. Appl. Thermal Eng. 17, 705–715.

Lazarek, G.M., Black, S.H., 1982. Evaporative heat transfer, pressure drop and critical heat flux in a small vertical tube with R-113. Int. J. Heat Mass Transfer 25 (7), 945–960.

Liu, Z., Winterton, R.H.S., 1991. A general correlation for saturated and subcooled flow boiling in tubes and annuli, based on a nucleate pool boiling equation. Int. J. Heat Mass Transfer 34, 1759–2766.

Moffat, R.J., 1985. Using uncertainty analysis in the planning of an experiment. J. Fluids Eng. 107, 173–178.

Neksa, P., Pettersen, J., 2001. Heat transfer and pressure drop of evaporating $CO_2$ in microchannels and system design implications of critical heat flux conditions. In: Proc. 2001 ASME International Mechanical Engineering Congress and Exposition, New York, AES-23631.

Pettersen, J., 2004. Flow vaporization of $CO_2$ in microchannel tubes. Exp. Thermal Fluid Sci. 28, 111–121.

Qu, W., Mudawar, I., 2003. Flow boiling heat transfer in two-phase micro-channel heat sinks—I. Experimental investigation and assessment of correlation methods. Int. J. Heat Mass Transfer 46, 2755–2771.

Sumith, B., Kaminaga, F., Matsumura, K., 2003. Saturated flow boiling of water in a vertical small diameter tube. Exp. Thermal Fluid Sci. 27, 789–801.

Tran, T.N., Wambsganss, M.W., France, D.M., 1995. Boiling heat transfer with three fluids in small circular and rectangular channels. ANL-95/9, Illinois.

Yan, Y.Y., Lin, T.F., 1998. Evaporation heat transfer and pressure drop of refrigerant R-134a in a small pipe. Int. J. Heat Mass Transfer 41, 4183–4194.

Yu, W., France, D.M., Wambsganss, M.W., Hull, J.R., 2002. Two-phase pressure drop, boiling heat transfer, and critical heat flux to water in a small-diameter horizontal tube. Int. J. Multiphase Flow 28, 927–941.

Yun, R., Kim, Y., 2003. Critical quality prediction for saturated flow boiling of $CO_2$ in horizontal small diameter tubes. Int. J. Heat Mass Transfer 46, 2527–2535.

Yun, R., Kim, Y., 2004. Flow regime transition criteria for horizontal two-phase flow of $CO_2$ in a heated narrow rectangular channel. Int. J. Multiphase Flow 30, 1259–1270.

Wambsganss, M.W., Jendrzejczyk, J.A., France, D.M., 1991. Two-phase flow patterns and transitions in a small, horizontal, rectangular channel. Int. J. Multiphase Flow 17 (3), 327–342.